www.czasopisma.pan.pl PAN www.journals.pan.pl
Chemical and Process Engineering 2022, 43 (1), 81–95
DOI: 10.24425/cpe.2022.140812

Biomimetic alginate/perfluorocarbon microcapsules – the effect on in vitro metabolic activity and long-term cell culture

Agata Stefanek[1,2*], Aleksandra Kulikowska-Darłak[1], Karolina Bogaj[1], Aleksandra Nowak[1], Joanna Dembska[1], Tomasz Ciach[1]

[1]Biomedical Engineering Laboratory, Faculty of Chemical and Process Engineering, Warsaw University of Technology, 00-645 Warsaw, Poland

[2]NanoSanguis S.A., Rakowiecka 36, 02-532 Warsaw, Poland

Cell encapsulation seems to be a promising tool in tissue engineering. However, it has been shown to have several limitations in terms of long-term cell cultures due to an insufficient oxygen supply. In this study we propose the use of novel microcapsules designed for long-term cell culture consisting of an alginate shell and perfluorocarbon (PFC) core, which works as a synthetic oxygen carrier and reservoir. The influence of PFC presence in the culture as well as the size of structures on cell metabolism was evaluated during 21-day cultures in normoxia and hypoxia. We showed significant improvement in cell metabolism in groups where cells were encapsulated in hydrogel structures with a PFC core. The cells maintained a typical metabolism (oxidative phosphorylation) through all 21 days of the culture, overcoming the oxygen supply shortage even in large structures (diameter > 1 mm). Applying PFC in alginate matrices can improve cell metabolism and adaptation in long-term cell cultures.

Keywords: alginate, microcapsules, cell culture, perfluorocarbons, metabolism

1. INTRODUCTION

Administration of encapsulated secretory cells is a promising therapy for metabolic diseases. Proper encapsulation should be tight and dense enough to offer protection from the immunological system but should also exhibit low mass transport resistance to ensure secretion products diffuse outside and nutrients remain inside the capsules. Unfortunately, there is a lack of techniques for long-term, three-dimensional cell encapsulation both in vivo and in vitro. The insufficient transport rate of oxygen and glucose inward to the 3D cell structures is the biggest obstacle for encapsulated cell culturing and implantation (Zhang et al., 2014). The aim of this work is to investigate the influence of the biomimetic hydrogel matrix containing a synthetic oxygen carrier used in long-term, three-dimensional in vitro cell culture on the viability, morphology (ability to create viable aggregates) and metabolism of cultured cells. The alginate beads and capsules are designed to mimic the naturally originated extracellular matrix (ECM), which is defined as an intricate network composed of extracellular macromolecules and minerals, such as collagen, enzymes, glycoproteins and hydroxyapatite organized in specific manner to provide structural and biochemical

* Corresponding author, e-mail: agata.stefanek.dokt@pw.edu.pl

support to surrounding cells (Theocharis et al., 2016; Yue, 2014). Moreover, the structure of the alginate provides free diffusion of nutrients inside the matrix and at the same time secretion of the metabolites of the encapsulated cells and immune system isolation (Dixit and Boelsterli, 2007). The synthetic oxygen carrier in the matrix is employed to face the widely reported problems appearing in 3D cell cultures, i.e. an insufficient oxygen level and the occurrence of necrotic zones in cell aggregates (Khattak et al., 2007). The project also includes investigation of the matrix composition influence on metabolism and proliferation during the culture. This allows us to distinguish critical factors for long-term viability and metabolic activity of the cultured cells in vitro.

Among all biomaterials for cell scaffolds there are those of natural origin, those of synthetic origin and specific structures created with decellularised natural ECM (Hoshiba et al., 2010). However, cell scaffolds often show insufficient biocompatibility, poor mechanical properties and cell growth conduction, and above all, do not provide a sufficient transport of nutrients to the cells, resulting in only short-term survival (Salvatori et al., 2017; Echeverria Molina et al., 2021). Among all strategies in utilizing scaffolds for tissue engineering there is only one where cells are encapsulated inside hydrogel structures of spherical geometry, which enables diffusion of the nutrients (oxygen, glucose) inside the microspheres and at the same time ensures immunoisolation of the encapsulated cells (El-Sherbiny and Yacoub, 2013). It is possible due to the fact that immunoglobulin molecules and antibodies are too big to diffuse into the hydrogel microspheres (Kanga et al., 2016). Moreover, hydrogel microspheres enable secretion of the molecules produced by the cells inside the microspheres (Figure 1) (Liu et al., 2013). This effect has a promising potential use in tissue engineering and regenerative medicine (Haisch et al., 2000). The immunoisolation provides for a wide range of applications in grafting cells obtained from extraneous donors, including interspecies grafts without the use of immunosuppressant drugs, and significantly decreases the risk of graft rejection (Figliuzzi et al., 2006). The mechanical properties of the hydrogel structures also allow their application as injectable scaffolds (de Vos et al., 2014).

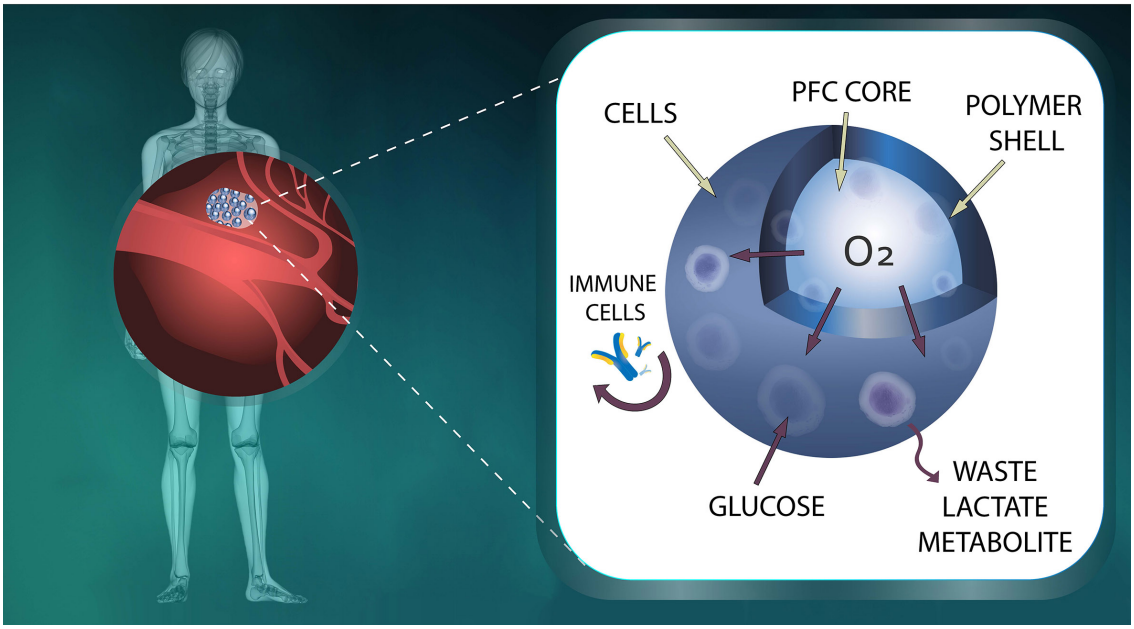

Fig. 1. Microcapsule with PFC core for long-term cell culture: the scheme of the design and functions

Cell encapsulation found many uses in tissue regeneration, especially in bone and cartilage reconstruction by the use of encapsulated stem cells, osteocytes and chondrocytes (Teixeira et al., 2012). This approach finds a wide application in the treatment of endocrine system diseases (diabetes, hypoparathyroidism), central nervous system dysfunctions (Parkinson's and Alzheimer's), as well as in the treatment of heart, liver and cancer diseases (Chen et al., 2007).

Numerous areas of drug delivery and tissue engineering have used alginate as a basic material for cell encapsulation, because its hydrated three-dimensional matrix enables cell adhesion, migration, proliferation and interaction with other cells. Alginate is a natural polysaccharide, commonly obtained from brown algae consisting of β-D mannuronate and α-L-guluronate connected in linear blocks. It is characterized by many advantages, including availability, easy and mild gelation method using polycations, and flexible parameters of the encapsulation process (alginate concentration and viscosity). Alginate microspheres were evaluated for Langerhans islets encapsulation, showed good immunoisolation properties and caused prolonged glucose homeostasis (Koch et al., 2003). The alginate was also employed in encapsulation and differentiation of embryonic bodies and individual stem cells in order to obtain their differentiation into hepatocytes (Wang et al., 2009; Farina et al., 2019).

Nowadays, one of the biggest challenges for cell encapsulation is to improve the long-term in vitro and in vivo stability of the hydrogel structures containing viable cells, and to develop an encapsulation method which enables to obtain structures of predictable interfacial transport properties. Encapsulated cells often experience an insufficient oxygen level to sustain long-term survival both in vitro and in vivo. As a result, local domains of necrotic and hypometabolic cells are formed. It has been reported that, for pancreatic islets, if the diameter of the encapsulated cell aggregate is higher than approximately 150 µm, the necrotic zones in the center of the aggregate occur due to nutrient competition. Necrotic cells release danger-associated molecular pattern molecules, which are potent activators of immune cells found in the transplantation site (de Vos et al., 2006). This phenomenon has been confirmed by our preliminary results. For this reason, more research dedicated to the basic physicochemical properties of hydrogel structures for cell encapsulation is necessary.

To improve the metabolic activity and viability of encapsulated cells, the application of synthetic oxygen carriers was investigated. Perfluorocarbons (PFC) have been applied in numerous biomedical and bioprocess systems, such as blood substitutes in clinical trials, gas permeable skin and wound protectants, dressings promoting wound healing by improving oxygen supply, as well as commercially available contrast agents for MRI and ultrasound imaging (Khattak et al., 2007; Pilarek, 2014; Wijekoon et al., 2013; Cosco et al., 2015). Specific systems incorporating PFC have been approved by the FDA for use in blood oxygenation during surgery (Krieger and Isom, 2012). It has been reported that the use of perfluorocarbons emulsified with alginate enhances viability of the encapsulated HepG2 cells. Applying PFC in cell encapsulation could improve cell viability by providing sufficient long-term oxygen supply both in vitro and in vivo due to the fact that PFC's may be able to 'reload' themselves with the oxygen from plasma due to the much greater oxygen solubility in the PFC (44 mM in PFOB) than in water (2.2 mM) (Khattak et al., 2007; Farris et al., 2016).

2. MATERIALS AND METHODS

Human liver HepG2 (hepatocellular carcinoma) cell line was obtained from American Type Culture Collection (ATCC® HB-8065™). In the presented studies, the HepG2 cell line was used as a continuation and comparison to the work of Khattak et al. (2007), who also used this cell line for encapsulation in beads made from alginate/PFOB emulsions.

2.1. Cell culture

HepG2 cell culture was maintained in MEM Alpha supplemented with 10% FBS, 1% Glutamine and 1% Pen-Strep in T-75 culture flask (all reagents from Gibco®, Thermo Fisher Scientific). Cell cultures were incubated at 37 °C, in a humidified atmosphere containing 5% CO_2 (Incubator Hera Cell 150, Thermo

Scientific). Cells were passaged every week by the use of 0.25% Trypsin-EDTA (Invitrogen). Fresh medium was used to resuspend cell pellets. The medium was changed every 3 days.

1.5% (w/v) alginate solution was prepared by mixing sodium alginate (216.12 g/mol) and 0.1% (w/v) glucose in PBS solution (all reagents from Sigma Aldrich). Alginate characterization: 20 000–40 000 cps (#MKBB8171, Sigma Aldrich). Gelling buffer consisted of 0.1 M calcium chloride (POCH), 0.1% (w/v) glucose and 10 mM HEPES (Sigma Aldrich). Washing buffer consisted of 10 mM calcium chloride, 0.9% (w/v) sodium chloride (Chempur), 0.1% (w/v) glucose and 10 mM HEPES. Perfluorooctylbromide (PFOB) was oxygenized for 1h with pure oxygen with a flow rate of 2 mL/min and connected to an encapsulator (B-395 Pro, BÜCHI, Switzerland) using 20 mL syringe with Luer Lock tip. PFOB was used as a model perfluorocarbon, in this study as an oxygen/carbon dioxide reservoir.

All solutions and reagents were sterilized using 0.22 μm filters (Stericup® and Steritop®, Merck Milipore) and prepared using MiliQ Water (Merck Milipore).

2.2. Encapsulation

After standard passage procedure, cells were divided into two parts: control cells that were seeded at the flat surface of a 24-well plate (5×10^5 cells/mL) and the second part, which was suspended in 1.5% alginate solutions (0.5×10^6 cells/mL) for encapsulation.

The encapsulation process was performed by the use of the encapsulator B-395 Pro (BÜCHI, Switzerland). To evaluate the influence of the size of the beads and capsules for encapsulated cells morphology, viability and metabolism, two groups of structures were produced: smaller (diameter app. 500 μm) and larger (diameter app. 1000 μm). 300/400 and 150/200 μm/μm concentric nozzles for microcapsule (MC) production and 400 and 200 μm nozzles for microsphere (MS) production were used. Two types of nozzles (regular and concentric) were used to produce beads and capsules (respectively, in both size groups) to evaluate the influence of perfluorocarbon presence on encapsulated cell morphology, viability and metabolism. The diameter of the structures produced with the use of a certain nozzle was approximately twice larger than the diameter of the nozzle. The diameters of the beads, capsules and the core of the capsules were measured using a confocal microscope (Zeiss LSM 880, Zeiss) and ZEN software. The PFC core's volume was calculated using the measured diameter.

To produce beads and capsules, both MC and MS, the laminar flow of the cell suspension (8.0 mL/min for 400 μm nozzle and 2.2 mL/min for 200 μm nozzle) was mechanically disturbed at a certain frequency (1000 Hz for 400 μm nozzle and 250 Hz for 200 μm nozzle), which resulted in uniform droplet formation. To produce MC, the syringe with oxidized PFOB was connected to the core nozzle and the alginate/cell suspension was connected to the shell nozzle, while for MS production, the core nozzle was blocked. During MC production the flow rate of PFOB was 8.0 mL/min for 400 μm nozzle and 2.2 mL/min for 200 μm nozzle. Hydrogel droplets were hardened in the gelling buffer after passing through the electrode, which electrostatically charged their surface to avoid aggregate formation (Figure 2). Gelling buffer was removed and MC/MS were washed with the washing buffer.

Approximately 250 μL of MC/MS was placed in each well of a 24-well plate. Washing buffer was removed and 1 mL of medium was added to each well. Control MS and MC without cells were produced as above, except that alginate solution without cells was used. Half of plates were placed in 37 °C, 5% CO_2 incubator. Second half of plates were placed in the hypoxic chamber (STEMCELL Technologies) and flashed with hypoxic gas mixture (1% O_2/5% CO_2/90% N_2) for 3h. The hypoxic chamber with plates was then hermetically closed and placed in 37 °C, 5% CO_2 incubator (NuAire). Hypoxic chamber allowed to create oxygen environment that is similar to the physiological one.

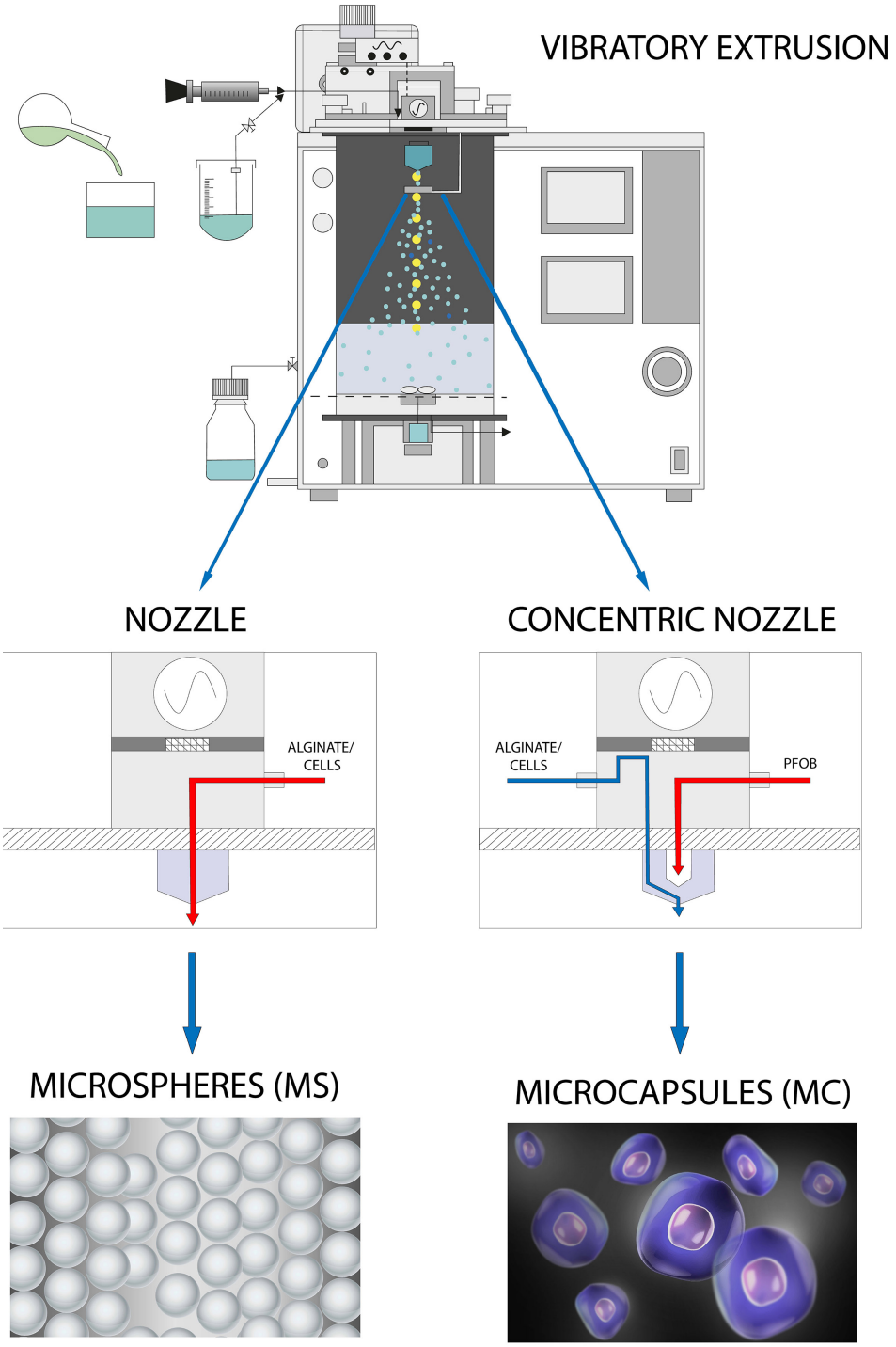

Fig. 2. Schematic presentation of the use of a single nozzle for the production of alginate microspheres and the concentric nozzle for the production of alginate microcapsules with PFC core during cell encapsulation

The medium was changed every 3 days. Every time hypoxic chamber was opened, it was flushed with hypoxic gas mixture by the use of gas mixer for at least 3 h. During the flashing the temperature was maintained at 37 °C.

After 1, 2, 7, 14 and 21 days, medium samples and cell lysates were collected in new plates and stored at –80 °C until analysis. Samples were collected from monolayer cell controls, MS/MC with cells and MS/MC without cells. Medium samples of half of the initial medium volume in a well (500 μL) were used for glucose and lactate analysis.

Cell lysates were prepared and collected for lactate dehydrogenase (LDH) and total protein content (BCA) analysis. Briefly, the remaining medium was removed and cells were washed with 1 mL of PBS solution. Then, 0.5 mL of 0.1 M sodium citrate (Sigma Aldrich) with 0.1 % (w/v) glucose in PBS solution was added to dissolve the microstructures. The plate was incubated at 37 °C for 10 min. To detached monolayer cells, 100 µL of trypsin-EDTA was added for each well. After incubation for 5 min at 37 °C, 400 µL of fresh medium was added to neutralize trypsin.

Both cells detached from the monolayer and cells from dissolved MC/MS were centrifuged (200 RCF, 5 min). Supernatant was removed. Cell residues were suspended in 250 µL of cold Pierce ™RIPA Buffer and incubated at 4 °C for 10 min to lyse the cells. Cell solutions were centrifuged (14 000 RCF, 15 min, 4 °C). Supernatant was collected and stored at –80 °C.

2.3. Live/Dead assay

For each time point, cell viability was monitored using the Live/Dead Cell Double Staining Kit (Sigma Aldrich; 04511 Cellstain double staining kit) or Live-Dead Cell Staining Kit (Abcam®; ab65470). The assay is based on membrane permeabilization discrimination of two dyes, which differentiate between live and dead cells. Photos were taken using the confocal microscope (Zeiss LSM 880, Zeiss).

2.4. Glucose assay

To determine the mass of consummated glucose, its concentration within medium samples was tested with a lab kit (BioMaxima SA). Analysis was carried out according to the manufacturer's protocol.

For all colorimetric tests, the absorbance measurements were taken using an Epoch Microplate Spectrophotometer (BioTek®). Plates were placed on the shaker during necessary incubations (Sky Line, ELMI).

2.5. Lactate assay

Medium samples were filtered (Amicon® Ultra-0.5 10K device – 10,000 NMWL Centrifugal Filter Devices, Merck Milipore) to prevent conversion of lactate acid to pyruvate in the presence of extracellular LDH that would lower the results. 20 µL of 100 x diluted filtrates were used to determine lactate acid concentration. MiliQ Water was used for dilutions. Colorimetric test with the aid of L-Lactate Assay Kit (Abcam®; ab65331) was conducted following the manufacturer's protocol.

2.6. LDH assay

Activity of intracellular LDH (lactate dehydrogenase) [mU/mL] was verified from cell lysates by the use of colorimetric Lactate Dehydrogenase Activity Assay Kit (Sigma Aldrich; Catalog Number MAK066). Samples were diluted with LDH Assay Buffer with dilution factor 2:3 or 3:2 (depending on the concentration of the samples). Further analysis was carried out according to the manufacturer's protocol.

2.7. BCA assay

Quantitation of total protein contents in the cell lysates was detected by the colorimetric test according to the manufacturer's protocol (Pierce™BCA Protein Assay Kit, Thermo Scientific; Catalog Number 23227).

2.8. Statistical analysis

Results of glucose, lactate and LDH concentration were calculated per proteins' mass in each sample. The results of parameters were compered between the groups and the statistical analysis was performed using 2-way ANOVA test in GraphPad Prism 7.05 software.

3. RESULTS

3.1. Stability of the structures

The method of hydrogel 3D structure production by the use of vibration extrusion was developed. The production process enables the creation of uniform solid microbeads or two phase microcapsules with a narrow size distribution with productivity (up to 5000 structures/min). The process parameters (flow rate through the nozzles, vibration frequency and electrode voltage) were chosen to obtain uniform structures and enable a fully controlled and reproducible process. By the use of a concentric nozzle, it was possible to obtain microcapsules with single or multiple PFC cores entrapped in the centre of the structure. Both beads and capsules were produced to evaluate the influence of the perfluorocarbon presence on encapsulated cell morphology, viability and metabolism.

Prepared microspheres (MS) and microcapsules (MC), remained stable during the 21-day cell culture. Beads were maintained in MEM/10% FBS during the entire duration of each experiment. The stability was evaluated by visual examination using light microscopy. There were no signs of hydrogel brakeage due to swelling, and also there was no PFC or cell leakage from the structures. The mean diameter of the produced structures for microspheres was 1047.79 ± 65.12 μm (400 μm nozzle) and 465.48 ± 53.30 μm (200 μm nozzle) and for microcapsules it was 1077.42 ± 113.69 μm (300/400 μm concentric nozzle) and 482.99 ± 61.06 μm (150/200 μm concentric nozzle). The mean diameter of the PFC core in the microcapsules was 621.68 ± 106.60 μm (300/400 μm concentric nozzle) and 376.56 ± 46.76 μm (150/200 μm concentric nozzle). The volume of the PFC core in the microcapsules was stable during the culture and there was no PFC evaporation from the microcapsules.

3.2. Cell viability

The Live/Dead staining test was performed to evaluate the distributions of viable and dead cells inside the beads and capsules and to monitor the cell density and morphology of cell aggregates. In general, viable cells can be observed in all experimental groups and for each time point, both in normoxia (Figure 3) and hypoxia (Figure 4), also at the end of the experiment, i.e. after 21 days of the culture. As shown qualitatively in Figures 3 and 4, we observed a drop of cell viability (the predominance of red stained cells over 24 h time point) 48 h after encapsulation, which can be interpreted as a cell response to encapsulation stress. The slight difference in cell viability can be observed for groups MS 400 and MC 300/400 in normoxia (the predominance of green stained cells in the group MC 300/400) suggesting the PFC core can reduce the encapsulation stress. Cells showed a tendency to create viable aggregates after approximately 7 days of culture (excluding group MS 400 both in hypoxia and normoxia – the aggregates were observed after 14 days of culture, mostly in normoxia, Figures 3 and 4). The cell aggregates in normoxia were larger compared to hypoxia, and the biggest viable aggregates were observed after 21 days in normoxic groups: MS 400, MC 150/200, and MC 300/400. It should be emphasized that cells prefer to grow in aggregates and for many types of cells only this form allows to achieve full functionality. However, culturing cell aggregates in vitro has limitations due to the insufficient nutrient transport. In this study, it was possible to

obtain viable cell aggregates even after 21 days of culture and to maintain the aerobic metabolism of cells, which may also result in maintaining the functionality of cells.

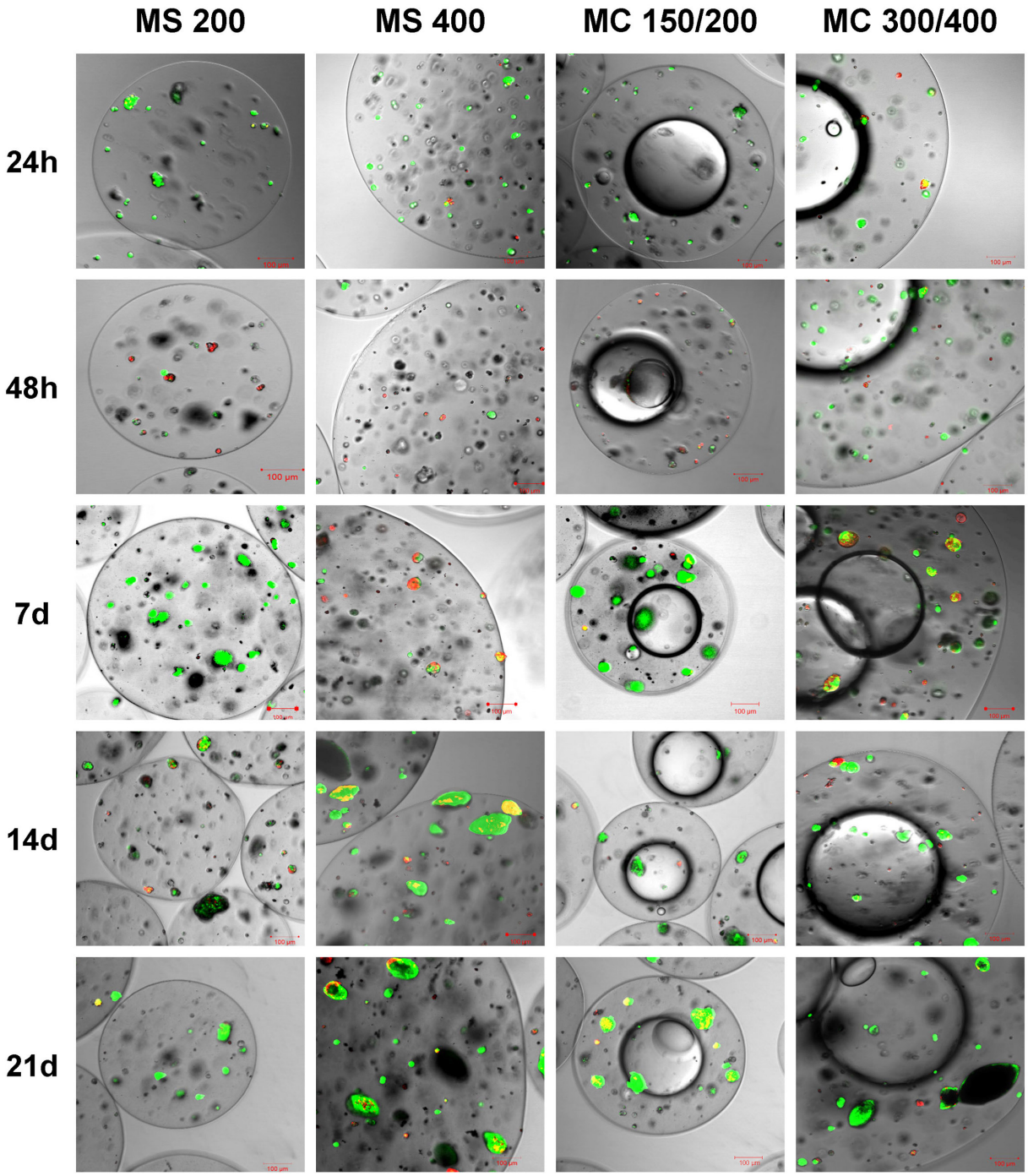

Fig. 3. Confocal microscope pictures of encapsulated cells cultured in normoxia, live/dead staining. Photos are grouped in columns representing structure type and size: microspheres 200 μm and 400 μm (MS 200 and MS 400) and microcapsules 200 μm and 400 μm (MC150/200 and MC 300/400).
The scale bars represent 100 micrometers (μm)

Live/Dead staining was also used to evaluate the location of viable/necrotic cells inside the hydrogel structure. There were no significant changes observed in terms of cell distribution. However the biggest viable cell aggregates were most often observed near the surface of the hydrogel structure as well as at the core/shell connection surface. The qualitative results of the Live/Dead staining tests show no significant differences between the groups in terms of viable cells amount and distribution.

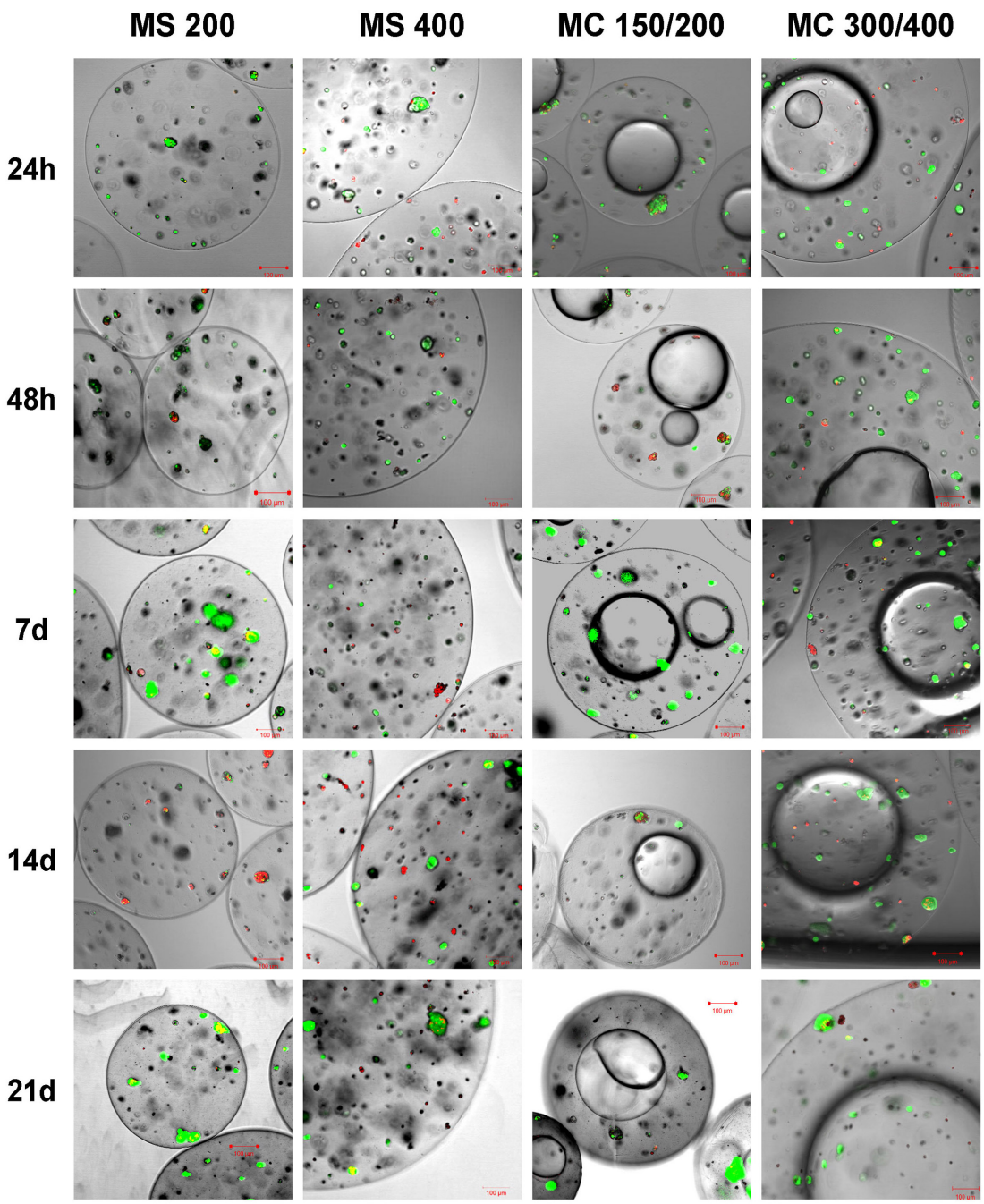

Fig. 4. Confocal microscope pictures of encapsulated cells cultured in hypoxia, live/dead staining. Photos are grouped in columns representing structure type and size: microspheres 200 μ and 400 μ (MS 200 and MS 400) and microcapsules 200 μ and 400 μ (MC150/200 and MC 300/400).
The scale bars represent 100 micrometers (μm)

3.3. Cell metabolism

Measurements of glucose, lactate and intracellular LDH levels were used to evaluate cell metabolism upon 21-day cell culture to confirm the hypothesis that oxygen supply covered by the addition of PFC into the hydrogel structure decreases glycolytic activity.

Cells cultured in the monolayer both in normoxia and hypoxia showed decreasing levels of glucose and increasing levels of lactate, while LDH levels remained low (except the 21 day time point in normoxia where we observed a significant increase of LDH levels over other groups, $p < 0.0001$). Data suggests

that both in hypoxia and normoxia the cell metabolism initially shifted to oxidative phosphorylation and switched to glycolysis over time with higher glycolytic activity at the end of 21-day culture in normoxia (Figures 5 and 6).

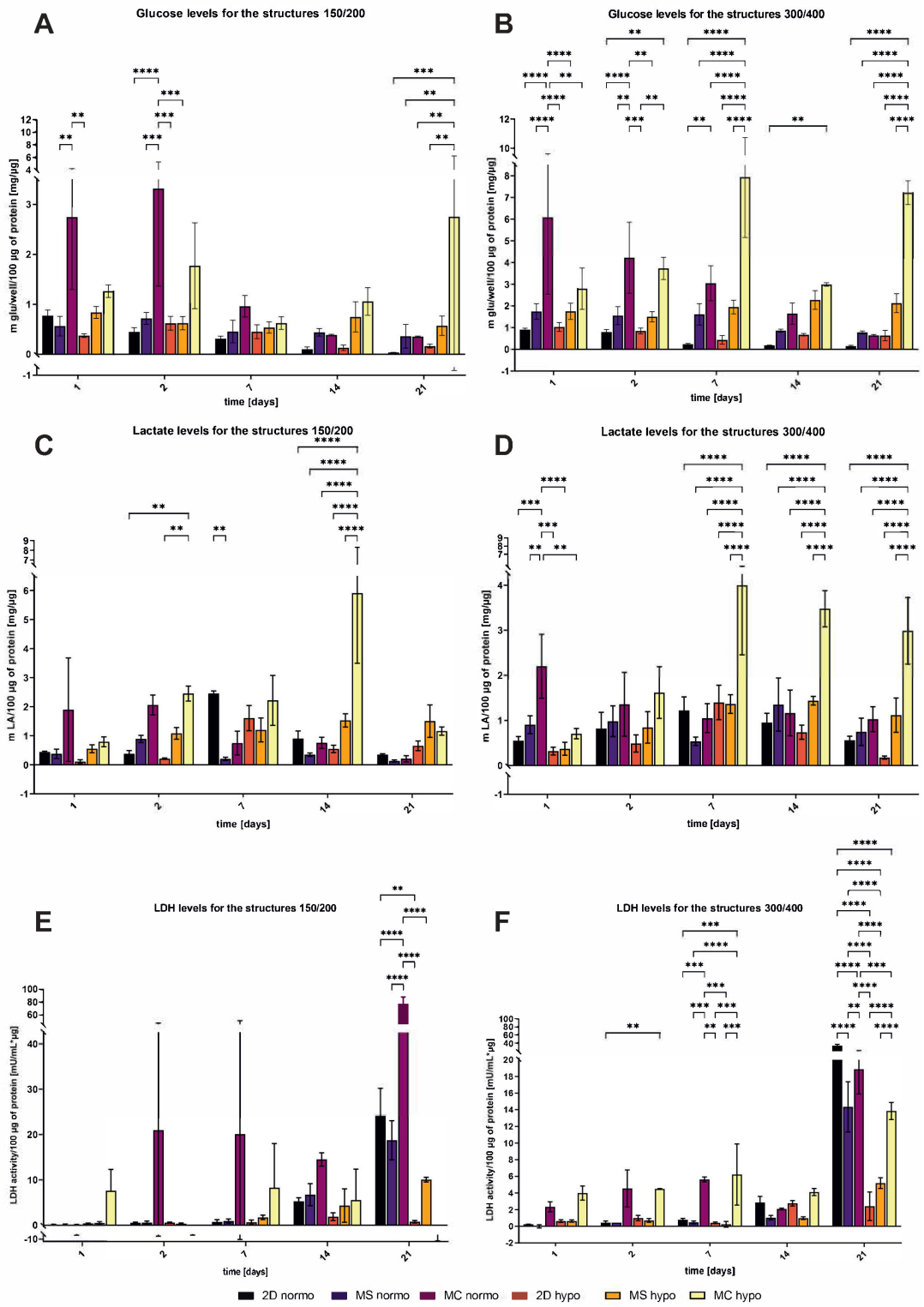

Fig. 5. Metabolic profiles of HepG2 cells encapsulated in microspheres and microcapsules with PFC core in different sizes cultured in normoxia and hypoxia. Metabolic activity of HepG2 cells tested by glucose, lactate, LDH, BCA assays. Glucose levels: A) structures 150/200 and B) structures 300/400; Lactate levels: C) structures 150/200 and D) structures 300/400; LDH levels: E) structures 150/200 and F) structures 300/400;
The significance levels are presented for P values < 0.01, where: ** represents $P < 0.01$, *** represents $P < 0.001$, and **** represents $P < 0.001$. P value were obtained using the 2-way ANOVA test

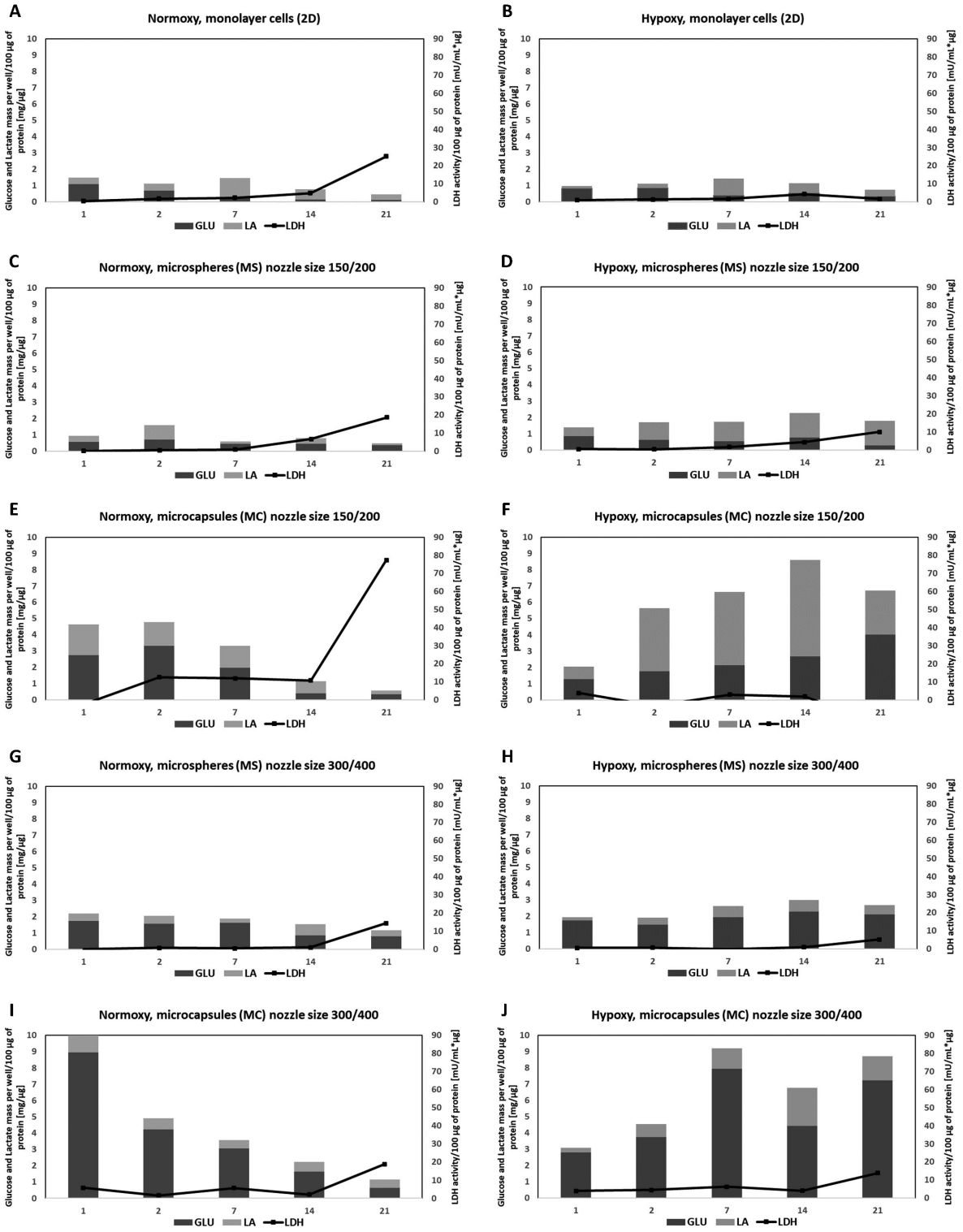

Fig. 6. Metabolic profiles of HepG2 cells encapsulated in microspheres and microcapsules with PFC cores in different sizes cultured in normoxia and hypoxia: monolayer cells (A, B), cells encapsulated in microspheres (C, D, G, H), cells encapsulated in microcapsules with PFC core (E, F, I, J)

An analogous metabolic effect can be observed for cells encapsulated in microspheres (without PFC core) cultured in normoxia. However, data collected for hypoxia shows strong glycolytic activity in all time points for MS 200 group (low level of glucose, high lactate) while for large structures we can observe a slowed metabolism (high level of glucose, low lactate, Figures 5 and 6).

Cells encapsulated in microcapsules cultured in normoxia show similar metabolic profiles to cells cultured in monolayers in normoxia: initial oxidative phosphorylation shifting to glycolysis over time with the higher glycolytic effect on 21st day of the culture ($p < 0.0001$, Figure 5). However, for hypoxic conditions the metabolic profiles for both small and large structures differ significantly from other groups ($p < 0.0001$) and show high levels of glucose, increasing levels of lactate and very low levels of intracellular LDH ($p < 0.0001$, Figures 5 and 6). Data suggests that in the hypoxic group (especially in the large group) cells maintained normal metabolism (oxidative phosphorylation) through all 21 days of the culture. These results prove that adding PFC can improve cell metabolism in long-term culture in large hydrogel structures, overcoming the shortage in oxygen supply. Probably, due to high oxygen solubility, PFC serves both as an oxygen reservoir at the beginning to avoid a rapid drop in oxygen supply to the cells, and also increases oxygen transport to the cells after encapsulation. This may happen due to an equalization of oxygen concentration inside the capsules and by the changing ratio of the outer surface area of the capsules to their active volume. It is also possible that the presence of PFC increases the diffusion rate of the oxygen in the hydrogel (due to the higher local difference in oxygen concentration).

4. DISCUSSION

A method of cell encapsulation in alginate hydrogel capsules with a liquid perfluorocarbon core was proposed. The idea of adding PFC to 3D hydrogel cell cultures was reported earlier (Khattak et al., 2007) although the design of the structures was significantly changed. Khattank et al. described cell culture in hydrogel microspheres made of alginate/PFC emulsion (W/O emulsion type). In such structures, the PFC micro and nano droplets may reduce the glucose diffusion in the entire sphere volume, since glucose is not soluble in PFC. The presence of PFC droplets decreases the area available for glucose diffusion and, on the other hand, increases oxygen diffusion. This phenomenon can result in slower cell growth, switching cell metabolism to glycolysis and cell necrosis especially in large structures (diameter > 1 mm). Therefore, we applied core (PFC)/shell (alginate) structures for cell encapsulation. We believe that a PFC core can maintain a physiological oxygen supply with no impact on glucose diffusion inside the hydrogel structure.

It has been reported that the diameter of spheres larger than 1 mm can negatively affect the rate of nutrient diffusion (Seifert and Phillips, 2008) and simultaneously, cell viability and metabolic activity. However, spheres larger than 1 mm are also found to be less immunogenic when transplanted into the body cavity (novel drug delivery systems or long-term secreting systems, (Veiseh et al., 2015)). Thus, finding the compromise between microsphere diameter and cell viability seems to be crucial for further development of drug delivery systems based on living cells.

The aim of applying biocompatible synthetic oxygen carriers into the hydrogel structures was to improve oxygen supply and create a reservoir for cells in long-term culture, which can maintain regular cell metabolism (ATP generation through oxidative phosphorylation). Cell metabolism was evaluated through measurements of the lactate, glucose and intracellular LDH levels over time. Oxidative phosphorylation can be distinguished through relatively high levels of glucose in the culture medium (close to initial glucose concentration), medium levels of lactate and low levels of LDH. Alternatively, low levels of glucose with simultaneous high levels of lactate and LDH can be interpreted as a switch in cell metabolism towards anaerobic glycolysis, which can occur in hypoxic conditions. This phenomenon is also characteristic for cancer cells, known as the Warburg effect (shift from ATP generation through oxidative phosphorylation to ATP generation through glycolysis even under normal oxygen conditions) (Cairns et al., 2011). This shift results in a high uptake of glucose since glycolysis is far less effective in terms of ATP generation from a glucose unit (36 ATPs generated from one unit of glucose through oxidative phosphorylation compared to 2 ATPs generated through glycolysis). However, it has been reported that the switch to glycolysis can

also occur in normally proliferating tissues with a sufficient oxygen supply. The anaerobic glycolysis can be a preferential metabolism for mammalian cells since it can generate a sufficient amount of ATP for proliferation (Vander Heiden et al., 2009).

The results of this study could have been influenced by the fact that the model cells used in these experiments were taken from the HepG2 cell line (cancer liver cells). As mentioned earlier, cancer cells can also choose anaerobic glycolysis as a preferential metabolism in normal oxygen conditions.

5. CONCLUSION

The results of this study showed a significant improvement of cell metabolism in a group where cells were encapsulated in hydrogel structures with a PFC core. Data showed that cells maintained normal metabolism (oxidative phosphorylation) through all 21 days of the culture, overcoming the oxygen supply shortage even in large structures (diameter > 1 mm). Applying PFC to hydrogel matrices can improve cell metabolism and adaptation in long-term cell cultures. Although further research is required including encapsulation of the non-cancer cells and animal model, such microencapsulation techniques can be considered for potential application in medicine when cells should be protected from the immunological system while maintaining normal metabolism and producing and releasing important substances like dopamine or insulin

We would like to acknowledge Polish National Science Centre for financial support (grant no. 2014/13/N/ST8/00098 and 2014/13/N/NZ5/013440).

REFERENCES

Cairns R.A., Harris I.S., Mak T.W., 2011. Regulation of cancer cell metabolism. *Nat. Rev. Cancer*, 11, 85–95. DOI: 10.1038/nrc2981.

Chen H., Ouyang W., Jones M., Metz T., Martoni C., Haque T., Cohen R., Lawuyi B., Prakash S., 2007. Preparation and characterization of novel polymeric microcapsules for live cell encapsulation and therapy. *Cell Biochem. Biophys.*, 47, 159–167. DOI: 10.1385/cbb:47:1:159.

Cosco D., Fattal E., Fresta M., Tsapis N., 2015. Perfluorocarbon-loaded micro and nanosystems for medical imaging: A state of the art. *J. Fluorine Chem.*, 171, 18–26. DOI: 10.1016/j.jfluchem.2014.10.013.

de Vos P., Faas M.M., Strand B., Calafiore R., 2006. Alginate-based microcapsules for immunoisolation of pancreatic islets. *Biomaterials*, 27, 5603–5617. DOI: 10.1016/j.biomaterials.2006.07.010.

de Vos P., Lazarjani H.A., Poncelet D., Faas M.M., 2014. Polymers in cell encapsulation from an enveloped cell perspective. *Adv. Drug Delivery Rev.*, 67–68, 15–34. DOI: 10.1016/j.addr.2013.11.005.

Dixit R., Boelsterli U.A., 2007. Healthy animals and animal models of human disease(s) in safety assessment of human pharmaceuticals, including therapeutic antibodies. *Drug Discovery Today*, 12, 336–342. DOI: 10.1016/j.drudis.2007.02.018.

Echeverria Molina M.I., Malollari K.G., Komvopoulos K., 2021. Design challenges in polymeric scaffolds for tissue engineering. *Front. Bioeng. Biotechnol.*, 9, 617141. DOI: 10.3389/fbioe.2021.617141.

El-Sherbiny I.M., Yacoub M.H., 2013. Hydrogel scaffolds for tissue engineering: Progress and challenges. *Global Cardiol. Sci. Pract.*, 2013, 38. DOI: 10.5339/gcsp.2013.38.

Farina M., Alexander J.F., Thekkedath U., Ferrari M., Grattoni A., 2019. Cell encapsulation: Overcoming barriers in cell transplantation in diabetes and beyond. *Adv. Drug Delivery Rev.*, 139, 92–115. DOI: 10.1016/j.addr.2018.04.018.

Farris A.L., Rindone A.N,, Grayson W.L., 2016. Oxygen delivering biomaterials for tissue engineering. *J. Mater. Chem. B*, 4, 3422–3432. DOI: 10.1039/c5tb02635k.

Figliuzzi M., Plati T., Cornolti R., Adobati F., Fagiani A., Rossi L., Remuzzi G., Remuzzi A., 2006. Biocompatibility and function of microencapsulated pancreatic islets. *Acta Biomater.*, 2, 221–227. DOI: 10.1016/j.actbio.2005.12.002.

Haisch A., Gröger A., Radke C., Ebmeyer J., Sudhoff H., Grasnick G., Jahnke V., Burmester G.R., Sittinger M., 2000. Macroencapsulation of human cartilage implants: Pilot study with polyelectrolyte complex membrane encapsulation. *Biomaterials*, 21, 1561–1566. DOI: 10.1016/S0142-9612(00)00038-7.

Hoshiba T., Lu H., Kawazoe N., Chen G., 2010. Decellularized matrices for tissue engineering. *Expert Opin. Biol. Ther.*, 10, 1717–1728. DOI: 10.1517/14712598.2010.534079.

Kanga A.R., Parka J.S., Ju J., Jeong G.S., Lee S.-H., 2016. Cell encapsulation via microtechnologies. *Biomaterials.*, 35, 2651–2663. DOI: 10.1016/j.biomaterials.2013.12.073.

Khattak S.F., Chin K.S., Bhatia S.R., Roberts S.C., 2007. Enhancing oxygen tension and cellular function in alginate cell encapsulation devices through the use of perfluorocarbons. *Biotechnol. Bioeng..*, 96, 156–166. DOI: 10.1002/bit.21151.

Koch S., Schwinger C., Kressler J., Heinzen Ch., Rainov N.G., 2003. Alginate encapsulation of genetically engineered mammalian cells: Comparison of production devices, methods and microcapsule characteristics. *J. Microencapsulation*, 20, 303–316. DOI: 10.1080/0265204021000058438.

Krieger K.H., Isom O.W., 2012. *Blood conservation in cardiac surgery*. Springer-Verlag New York, Inc., 588–592.

Liu J., Xu H.K., Zhou H., Weir M.D., Chen Q., Trotman C.A., 2013. Human umbilical cord stem cell encapsulation in novel macroporous and injectable fibrin for muscle tissue engineering. *Acta Biomater.*, 9, 4688–4697. DOI: 10.1016/j.actbio.2012.08.009.

Pilarek M., 2014. Liquid perfluorochemicals as flexible and efficient gas carriers applied in bioprocess engineering: An updated overview and future prospects. *Chem. Process Eng.*, 35, 463–487. DOI: 10.2478/cpe-2014-0035.

Salvatori M., Katari R., Patel T., Peloso A., Mugweru J., Owusu K., Orlando G., 2017. Extracellular matrix scaffold technology for bioartificial pancreas engineering: State of the art and future challenges. *J. Diabetes Sci. Technol.*, 8, 159–169. DOI: 10.1177/1932296813519558.

Seifert B.D., Phillips J.A., 2008. Production of small, monodispersed alginate beads for cell immobilization. *Biotechnol. Progr.*, 13, 562–568. DOI: 10.1021/bp9700723.

Teixeira L.S. M., Feijen J., van Blitterswijk C.A., Dijkstra P.J., Karperien M., 2012. Enzyme-catalyzed crosslinkable hydrogels: Emerging strategies for tissue engineering. *Biomaterials*, 33, 1281–1290. DOI: 10.1016/j.biomaterials.2011.10.067.

Theocharis A.D., Skandalis S.S., Gialeli C., Karamanos N.K., 2016. Extracellular matrix structure. *Adv. Drug Delivery Rev.*, 97, 4–27. DOI: 10.1016/j.addr.2015.11.001.

Vander Heiden M.V., Cantley L.C., Thompson C.B., 2009. Understanding the Warburg effect: The metabolic requirements of cell proliferation. *Science*, 324, 1029–1033. DOI: 10.1126/science.1160809.

Veiseh O., Doloff J.C., Ma M., Vegas A.J., Tam H.H., Bader A.R., Li J., Langan E., Wyckoff J., Loo W.S., Jhunjhunwala S., Chiu A., Siebert S., Tang K., Hollister-Lock J., Aresta-Dasilva S., Bochenek M., Mendoza-Elias J., Wang Y., Qi M., Lavin D.M., Chen M., Dholakia N., Thakrar R., Lacík I., Weir G.C., Oberholzer J., Greiner D.L., Langer R., Anderson D.G., 2015. Size- and shape-dependent foreign body immune response to materials implanted in rodents and non-human primates. *Nature Mater.* 14, 643–651. DOI: 10.1038/nmat4290.

Wang N., Adams G., Buttery L., Falcoone F. H., Stolnik S., 2009. Alginate encapsulation technology supports embryonic stem cells differentiation into insulin-producing cells. *J. Biotechnol.*, 144, 304–312. DOI: 10.1016/j.jbiotec.2009.08.008.

Wijekoon A., Fountas-Davis N., Leipzig N.D., 2013. Fluorinated methacrylamide chitosan hydrogel systems as adaptable oxygen carriers for wound healing. *Acta Biomater.*, 9, 5653–5664. DOI: 10.1016/j.actbio.2012.10.034.

Yue B., 2014. Biology of the extracellular matrix: An overview. *J. Glaucoma.*, 23, S20–S23. DOI: 10.1097/IJG.0000000000000108.

Zhang Q., Lu H., Kawazoe N., Chen G., 2014. Pore size effect of collagen scaffolds on cartilage regeneration. *Acta Biomaterialia.*, 10, 2005–2013. DOI: 10.1016/j.actbio.2013.12.042.

Received 02 February 2022
Received in revised form 14 March 2022
Accepted 14 March 2022